Journal of Modern Optics

ISSN: 0950-0340 (Print) 1362-3044 (Online) Journal homepage: https://www.tandfonline.com/loi/tmop20

# A Generalized Fourier-based Method for the Analysis of 2D Moiré Envelope-forms in Screen Superpositions

Isaac Amidror

**To cite this article:** Isaac Amidror (1994) A Generalized Fourier-based Method for the Analysis of 2D Moiré Envelope-forms in Screen Superpositions, Journal of Modern Optics, 41:9, 1837-1862, DOI: 10.1080/09500349414551761

**To link to this article:** https://doi.org/10.1080/09500349414551761

Published online: 01 Mar 2007.

JOURNAL OF MODERN OPTICS, 1994, VOL. 41, NO. 9, 1837–1862

# A generalized Fourier-based method for the analysis of 2D Moiré envelope-forms in screen superpositions

ISAAC AMIDROR

Peripheral Systems Laboratory (LSP),
Swiss Federal Institute of Technology (EPFL),
1015 Lausanne, Switzerland

(*Received 14 February 1994 and accepted 25 April 1994*)

**Abstract.** When repetitive structures such as line-gratings or dot-screens are superposed, a new pattern may become clearly visible in the superposition, although it does not exist in any of the original structures. This phenomenon, which in some cases appears to be very spectacular, is known as the superposition Moiré effect. In this article we analyse the 2D envelope-forms of these Moiré patterns, based on the Fourier theory, and we show how they can be derived analytically from the original superposed structures, either in the spectral domain or directly in the image domain. This approach not only offers a qualitative geometric analysis of each superposition Moiré, but also enables the intensity levels of each Moiré to be determined quantitatively. We first develop this analysis method for the simple case of line-grating superpositions, and then we generalize it to the superposition of doubly periodic structures such as dot screens, for any order Moiré. We finally show how, by means of this analysis method, we can fully explain (and predict) the surprising envelope-forms generated in the superpositions of screens with any desired dot-shapes, for any order of Moiré.

## 1. Introduction

The superposition Moiré is a well-known phenomenon which occurs when periodic or quasi-periodic structures (such as line-gratings, dot-screens, etc.) are superposed. It consists of a visible pattern which is clearly observed at the superposition, although it does not appear in any of the original structures [1]. The Moiré effect between superposed structures occurs because of the geometric distribution of dark and bright areas in the superposed image: areas in which dark elements of the original structures cross each other contain less black than areas where the original structure elements fall between each other and fill the white spaces better.

Although the basic geometric properties of the Moiré patterns can be found using simple geometric or algebraic approaches [2–5], it has been shown that the best approach for exploring the Moiré phenomenon is the spectral approach, which is based on the Fourier theory [6]. Unlike the geometric and the algebraic methods, this approach enables us to analyse properties not only in the original images and in their superposition but also in their spectral representations, and thus it offers a more profound insight into the problem and provides indispensable tools for exploring it. Moreover, the additional dimension offered by the impulse amplitudes in the spectrum (in addition to their geometric locations) also enables a quantitative

analysis of the Moiré intensity levels, in addition to the qualitative geometric analysis of the Moiré, already offered by the earlier approaches.

In this article we will concentrate on the analysis of the envelope-form and the intensity levels of Moiré patterns which are obtained in the superposition of periodic dot-screens (such as halftone screen films of the type used in the printing world for producing grey level images). As shown in figure 1, such screen superpositions may result in very spectacular Moiré patterns, which are even more striking when the superposed screens (films) are slowly moved on top of each other. Based on the Fourier approach, we will introduce a generalized method for extracting the intensity profile (or the envelope-form) of such superposition Moirés: first between line-gratings (in section 3), and then (in section 4) between general two-dimensional (2D) periodic structures, such as dot-screens with any desired dot-shapes. Extending the duality between the image and the spectral domains to include Moiré-envelopes as well, we will show how the extraction of the Moiré-envelope can be interpreted in either of these two domains. We will also see how results which have previously been derived using quite complicated mathematical methods can easily be obtained for any periodic screens as a simple special case of our approach. Finally, we will show (in sections 5 and 6) how this analysis method fully explains the surprising envelope-forms of the Moiré patterns obtained between screens of any desired dot shapes, including in the case of higher-order Moirés.

## 2. Background

In this article we concentrate on 2D images in the $(x, y)$ plane and their 2D spectra in the $(u, v)$ plane, which are obtained by the 2D Fourier transform. In fact, we restrict ourselves only to some specific types of 2D images, such as line-gratings or dot-screens; in this section we list the basic properties of the image types we are concerned with, and review the implications of these properties both in the image and in the spectral domains.

First, we only deal here with monochromatic (black and white) images. In this case each image can be represented by a *reflectance* function, which assigns to any point $(x, y)$ of the image a value between 0 and 1 representing its light reflectance: 0 for black (i.e. no reflected light), 1 for white (i.e. full light reflectance), and intermediate values for in-between shades. In the case of transparencies, the reflectance function is replaced by a *transmittance* function defined in a similar way. Since the superposition of black and any other shade always gives black, this suggests a *multiplicative* model for the superposition of monochromatic images. Thus, when $N$ monochromatic images are superposed, the reflectance of the resulting image is given by the *product* of the reflectance functions of the individual images:

$$r(x, y) = r_1(x, y)r_2(x, y)\ldots r_N(x, y). \tag{1}$$

If we denote the Fourier transform of each function by the respective capital letter and the 2D convolution by $**$, we get using the convolution theorem [7, p. 18, 8, p. 244]

$$R(u, v) = R_1(u, v)**R_2(u, v)**\ldots** R_N(u, v). \tag{2}$$

Second, we are basically interested in *periodic* images defined on the continuous $(x, y)$ plane, such as line gratings or dot screens, and their superpositions. This implies that the image spectrum in the $(u, v)$ plane is a 2D *nailbed* of discrete impulses, given by the Fourier series decomposition of the image [8, p. 204]. In the

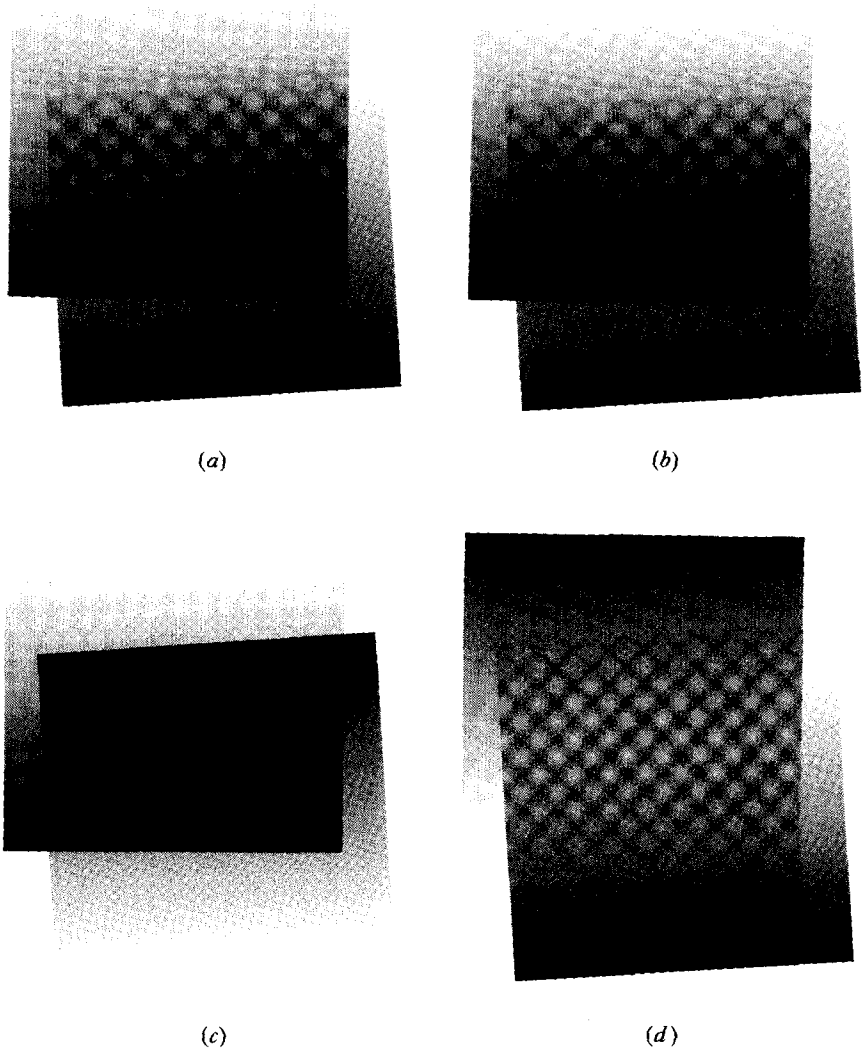


Figure 1. The superposition of binary (B/W) dot-screens may yield Moiré effects with spectacular envelope-forms. This figure demonstrates that the shape and the surface of the screen dots only affect the shape and the intensity levels of the Moiré-envelope; but the period and the direction of the Moiré remain unchanged (unless the angles and frequencies of the superposed screens are modified). In all the cases (*a*)–(*d*), two screens with identical frequencies and gradually increasing dots are superposed with the same angle difference of 4°; this implies that in all of the cases the Moiré in question is a (1, 0, −1, 0) Moiré. (*a*) Two screens with black circular dots; (*b*) top screen with black circular dots and bottom screen with black square dots; (*c*) top screen with black triangular dots and bottom screen with black circular dots; (*d*) top screen with black square dots and bottom screen with black circular dots.

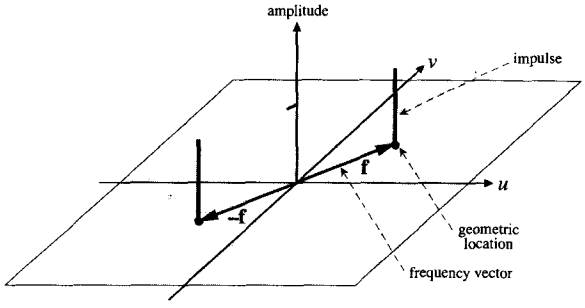


Figure 2. The *geometric location* and *amplitude* of impulses in the 2D spectrum. To each impulse is attached its *frequency vector*, which points to the geometric location of the impulse in the spectrum plane $(u, v)$.

case of line gratings, the nailbed is reduced to a one-dimensional (1D) *comb* of impulses in the $(u, v)$ plane. A strong impulse in the spectrum indicates a pronounced periodic component in the original image at the frequency and direction of that impulse.

Each impulse in the 2D spectrum is characterized by two properties: its *geometric location* (or *impulse location*), and its *amplitude* (see figure 2). To the geometric location of any impulse is attached a *frequency vector* $\mathbf{f}$ in the spectrum plane, which connects the spectrum origin with the geometric location of the impulse. This vector can be expressed either by its polar coordinates $(f, \alpha)$, where $\alpha$ is the direction of the impulse and $f$ is its distance from the origin (i.e. its frequency in that direction); or by its Cartesian coordinates $(f_u, f_v)$, where $f_u$ and $f_v$ are the horizontal and vertical components of the frequency. In terms of the original image, the *geometric location* of an impulse in the spectrum determines the frequency $f$ and the direction $\alpha$ of the corresponding periodic component in the image, and the *amplitude* of the impulse represents the intensity of that periodic component in the image. (Note that if the original image is not symmetric about its origin, the amplitude of each impulse in the spectrum may also have a non-zero imaginary component.)

However, the question whether or not an impulse in the spectrum represents a visible periodic component in the image strongly depends on properties of the human visual system. The fact that the eye cannot distinguish fine details above a certain frequency (i.e. below a certain period) suggests that the human visual system model includes a low-pass filtering stage. This is a bidimensional bell-shaped filter whose form is anisotropic (since it appears that the eye is less sensitive to small details in diagonal directions such as 45° [9, pp. 79–84]). However, for the sake of simplicity this low-pass filter can be approximated by the *visibility circle*, a circular step function around the spectrum origin whose radius represents the *cut-off frequency* (i.e. the threshold frequency beyond which fine detail is no longer detected by the eye). Obviously, its radius depends on several factors such as the contrast of the observed details, the viewing distance, light conditions, etc. If the frequencies of the original image elements are beyond the border of the visibility circle in the spectrum, the eye cannot see them; but if a strong enough impulse in the spectrum of the image superposition falls inside the visibility circle, then a Moiré effect becomes visible in the superposed image.

The Moiré patterns obtained in the superposition of periodic structures such as line gratings or dot-screens can be described at two different levels. The first, basic

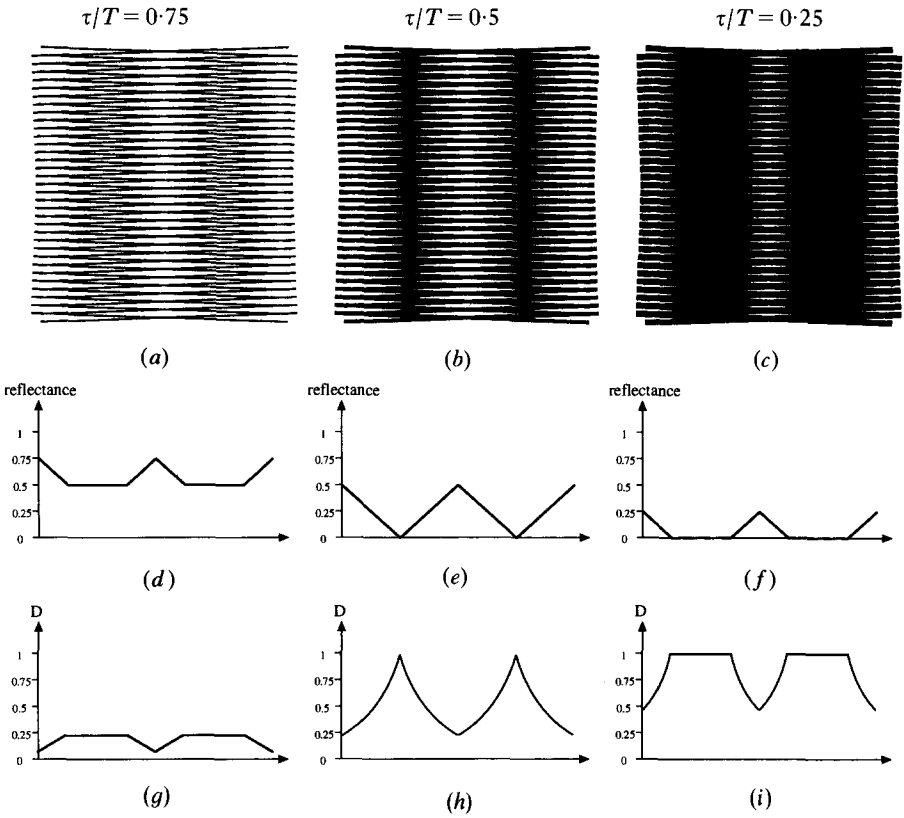


Figure 3. A (1, −1) Moiré between two identical binary gratings with the same periods and angles and with opening ratios (i.e. white-width/period ratios) of: (*a*) 0·75; (*b*) 0·5; (*c*) 0·25. (*d*), (*e*) and (*f*) show the respective Moiré profiles in terms of *reflectance*, as received from the mathematical model. (*g*), (*h*) and (*i*) show the same Moiré profiles after their adaptation to the human visual perception, i.e. in terms of logarithmic *density*.

level only considers the planar properties (*periods* or *frequencies* and *angles*) of the repetitive structures in the original images and in the produced Moiré patterns. The second level also includes the *amplitude* properties of the original structures and of their Moiré patterns, which can be added to their planar 2D description as a third dimension, describing their intensity or grey-level variations. This three-dimensional (3D) description of the Moiré is called its *intensity profile* or *envelope-form*. Note that the term *profile* originates from the simple Moiré case obtained in the superposition of two line-gratings (see figure 3), in which a 1D plot describing the projection of the Moiré-bands on a perpendicular plane is enough to describe the form (profile) of the Moiré. However, in more complex cases where the Moiré forms are no longer simple bands, the term *envelope* is more appropriate for describing the shape and the intensity variations of the Moiré pattern.

According to the convolution theorem (equations (1), (2)), when $N$ line-gratings are superposed in the image domain, the resulting spectrum is the convolution of their individual spectra. This comb (or nailbed) convolution can be seen as an operation in which frequency vectors of the individual spectra are added vectorially, while the corresponding impulse amplitudes are multiplied. More precisely, each

impulse in the spectrum-convolution is generated during the convolution process by the contribution of *one* impulse from *each* individual spectrum: its location is given by the sum of their frequency vectors, and its amplitude is given by the product of their amplitudes. This permits us to introduce an indexing method for denoting each of the impulses of the spectrum-convolution in a unique, unambiguous way. The general impulse in the spectrum-convolution will be denoted the $(k_1, k_2, \ldots, k_N)$ *impulse*, where $k_i$ is the index (harmonic), within the comb of the $i$th spectrum, of the impulse that this $i$th spectrum contributed to the convolution. Using this formal notation we therefore have the following result:

The geometric location of the general $(k_1, k_2, \ldots, k_N)$ impulse in the spectrum-convolution is given by the vectorial sum (or linear combination)

$$\mathbf{f}_{k_1,k_2,\ldots,k_N} = k_1\mathbf{f}_1 + k_2\mathbf{f}_2 + \ldots + k_N\mathbf{f}_N, \tag{3}$$

and its amplitude is given by

$$a_{k_1,k_2,\ldots,k_N} = a_{k_1}^{(1)} a_{k_2}^{(2)} \ldots a_{k_N}^{(N)}, \tag{4}$$

where $\mathbf{f}_i$ denotes the frequency vector of the fundamental impulse in the spectrum of the $i$th grating, and $k_i\mathbf{f}_i$ and $a_{k_i}^{(i)}$ are respectively the frequency vector and the amplitude of the $k_i$th harmonic impulse in the spectrum of the $i$th grating.

The vectorial sum of equation (3) can also be written in terms of its Cartesian components. If $f_i$ are the frequencies of the $N$ original gratings and $\theta_i$ are the angles that they form with the positive horizontal axis, then the coordinates $(f_u, f_v)$ of the $(k_1, k_2, \ldots, k_N)$ impulse in the spectrum-convolution are given by

$$\left.\begin{aligned} f_u{}^{k_1,k_2,\ldots,k_N} &= k_1 f_1 \cos\theta_1 + k_2 f_2 \cos\theta_2 + \ldots + k_N f_N \cos\theta_N, \\ f_v{}^{k_1,k_2,\ldots,k_N} &= k_1 f_1 \sin\theta_1 + k_2 f_2 \sin\theta_2 + \ldots + k_N f_N \sin\theta_N. \end{aligned}\right\} \tag{5}$$

Therefore, the frequency, the period and the angle of the considered impulse (and of the Moiré it represents) are given by the length and the direction of the vector $\mathbf{f}_{k_1,k_2,\ldots,k_N}$, as follows:

$$f = (f_u^2 + f_v^2)^{1/2}, \quad T_M = 1/f, \quad \varphi_M = \arctan(f_v/f_u). \tag{6}$$

Note that in the special case of $N = 2$ gratings, when a Moiré effect occurs due to the $(1, -1)$-impulse in the convolution, equations (5)–(6) are reduced to the familiar geometrically obtained formulas of the period and angle of the Moiré effect between two gratings [2, 5]

$$T_M = \frac{T_1 T_2}{(T_1^2 + T_2^2 - 2T_1T_2\cos\alpha)^{1/2}}, \quad \sin\varphi_M = \frac{T_1 \sin\alpha}{(T_1^2 + T_2^2 - 2T_1T_2\cos\alpha)^{1/2}}, \tag{7}$$

(where $T_1$ and $T_2$ are the periods of the two original gratings and $\alpha$ is the angle difference between them, $\theta_1 - \theta_2$). When $T_1 = T_2$ this is further simplified into the well-known formulas [1, 3]

$$T_M = \frac{T}{2\sin(\alpha/2)}, \quad \varphi_M = 90° - \alpha/2. \tag{8}$$

Finally, a word about the notations used for the superposition Moirés. In this article we use a systematic notational formalism, which provides an unambiguous means for identifying the various Moiré effects. As we have seen, a $(k_1, k_2, \ldots, k_N)$ impulse in the spectrum-convolution which falls close to the spectrum origin, inside the visibility circle, represents a Moiré effect in the superposed image. We call the $N$-grating Moiré whose fundamental impulse is the $(k_1, k_2, \ldots, k_N)$ impulse in

the spectrum-convolution a $(k_1, k_2, \ldots, k_N)$ *Moiré*; the highest absolute value in the index-list is called the *order* of the Moiré. Note that in the case of doubly periodic images, such as in regular dot screens, each superposed image contributes two perpendicular frequency vectors to the spectrum, so that in equations (3)–(5) above $N$ should be replaced by $2N$ (twice the number of superposed images).

## 3. Extraction of the profile of a Moiré between superposed line-gratings

Assume that we are given two line-gratings (see figure 4). The spectrum of each of these line-gratings consists of an infinite impulse-comb, in which the amplitude of the $k$th impulse is given by the coefficient of the $k$-harmonic term in the Fourier series development of that line-grating. When we superpose (i.e. multiply) these two line-gratings the spectrum of the superposition is, according to the convolution theorem, the convolution of the two original combs, which gives an oblique nailbed of impulses (figure 4($f$)). Each Moiré which appears in the superposition of the gratings is represented in the spectrum of the superposition by a comb of impulses which is generated in the convolution of the combs of the original line-gratings. If a Moiré in the superposition is visible, it means that in the spectral domain the fundamental impulse-pair of the Moiré comb is located inside the visibility circle, close to the spectrum origin; this impulse determines the period and the direction of the Moiré. Now, by extracting from the spectrum convolution only this infinite Moiré comb and taking its inverse Fourier transform, we can reconstruct, back in the image domain, the isolated contribution of the Moiré in question to the image superposition; this is the intensity profile (or envelope form) of the Moiré (see figure 4($g$), ($h$)). In the present section we will see in detail how the profile of any Moiré between superposed line-gratings can be extracted, either from the spectral domain, or directly from the image domain.

Let us denote by $c_n$ the amplitude of the $n$th impulse of the Moiré comb. If the Moiré in question is a $(k_1, k_2)$ Moiré, the fundamental impulse of its comb is the $(k_1, k_2)$ impulse in the spectrum convolution, and the $n$th impulse of its comb is the $(nk_1, nk_2)$ impulse in the spectrum convolution. Therefore we have

$$c_n = a_{nk_1, nk_2},$$

and according to equation (4) we get

$$c_n = a^{(1)}_{nk_1} a^{(2)}_{nk_2},$$

where $a^{(1)}_i$ and $a^{(2)}_i$ are the respective impulse amplitudes from the combs of the first and of the second line-gratings. In other words, we can say:

*Result* 3.1

The impulse amplitudes of the Moiré comb in the spectrum convolution are received by a simple term-by-term multiplication of the combs of the original superposed gratings (or subcombs thereof, in case of higher-order Moirés).

For example, in the case of a $(1, -1)$ Moiré (as in figure 4($f$)) the amplitudes of the Moiré comb impulses are given by: $c_n = a_{n,-n} = a^{(1)}_n a^{(2)}_{-n}$ and in the case of the second-order $(1, -2)$ Moiré (see figure 5) the impulse amplitudes of the Moiré comb are given by: $c_n = a_{n,-2n} = a^{(1)}_n a^{(2)}_{-2n}$ (note that if the original gratings are symmetric about the origin, then $a^{(2)}_{-i} = a^{(2)}_i$). Now, since we know also the exact *locations* of the impulses of the Moiré comb (according to equation (3)), the spectrum of the isolated Moiré in question is fully determined, and we can therefore reconstruct, back

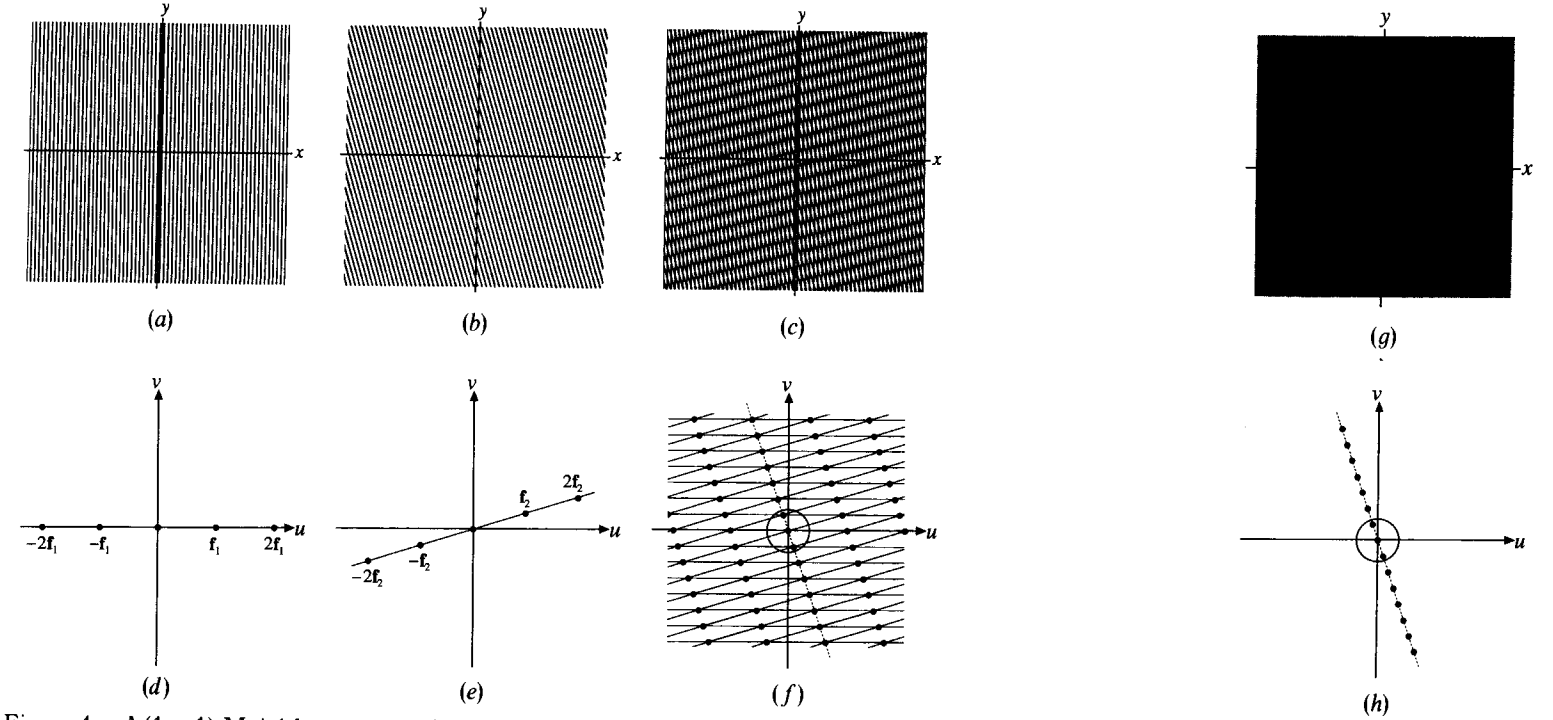


Figure 4. A $(1, -1)$ Moiré between two binary gratings in the image domain and its representation in the spectral domain. (*a*), (*b*) and (*c*) show two binary gratings and their superposition in the image domain; their respective spectra are the infinite combs shown in (*d*) and (*e*) and their convolution (*f*). Black dots in the spectra indicate the geometric location of the impulses; the straight lines connecting them have been added only in order to clarify the geometric relations. The circle in the centre of the spectrum (*f*) represents the visibility circle. It contains the impulse pair whose frequency vectors are $\mathbf{f}_1 - \mathbf{f}_2$ and $\mathbf{f}_2 - \mathbf{f}_1$; this is the fundamental impulse pair of the Moiré seen in (*c*). The dotted line in (*f*) shows the infinite comb of impulses which represents the $(1, -1)$ Moiré. (*h*) shows the spectrum of the isolated $(1, -1)$ Moiré comb after its extraction from the full spectrum (*f*). The impulse amplitudes of this comb are the term-by-term products of the respective impulse amplitudes from the combs (*d*) and (*e*). (*g*) Shows the image-domain function which corresponds to the spectrum (*h*). This is the profile (or envelope) of the $(1, -1)$ Moiré shown in (*c*); its crests are triangular (or trapezoidal), as shown in figure 3 (*d*)–(*f*).

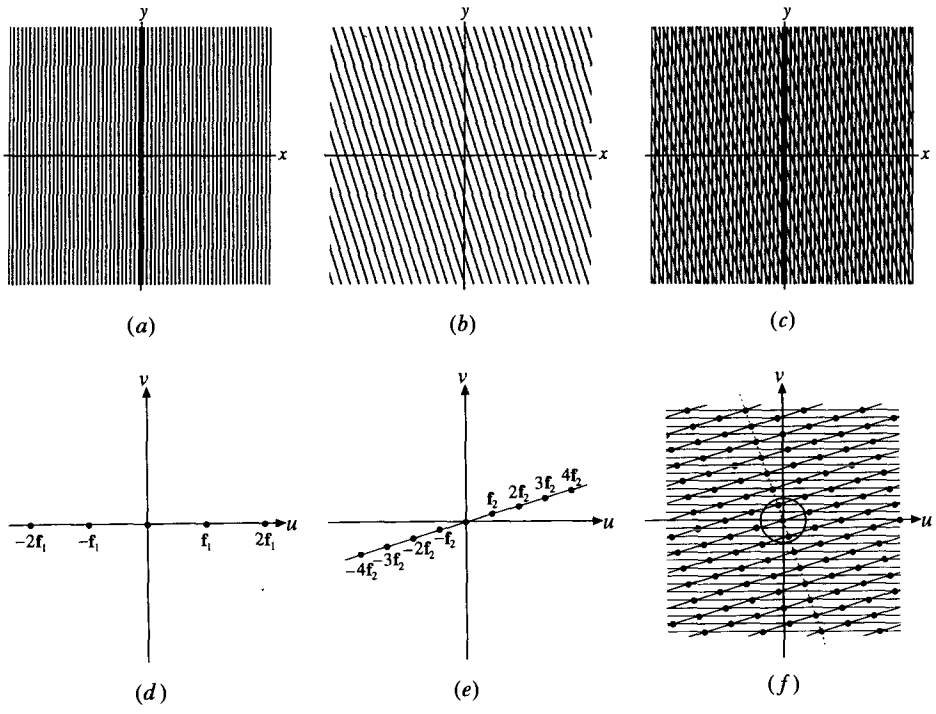


Figure 5. Binary gratings (*a*) and (*b*) as in figure 4 but with (*b*) having half the frequency, and their superposition (*c*); (*d*), (*e*) and (*f*) are their respective spectra. The visibility circle in the centre of the spectrum (*f*) contains the impulses with frequency vectors $\mathbf{f}_1 - 2\mathbf{f}_2$ and $2\mathbf{f}_2 - \mathbf{f}_1$, which originate from the second harmonic of $\mathbf{f}_2$, and represent the fundamental impulse pair of the Moiré. Note that the Moiré seen in (*c*) is a $(1, -2)$ Moiré, but it still has the same angle and frequency as the $(1, -1)$ Moiré of figure 4, and only its intensity is weaker.

in the image domain, the profile (envelope form) of the Moiré. This can be done, formally speaking, by taking the inverse Fourier transform (FT) of the isolated Moiré comb. Practically, this can be done either by interpreting the Moiré comb as a Fourier series development, and reconstructing the Moiré profile it represents in the image domain by summing up the corresponding sinusoidal functions (up to the desired precision); or, more efficiently, by approximating the continuous inverse FT of the isolated Moiré comb by means of the inverse discrete FT (using fast FT).

Result 3.1 was already discovered by Patorski *et al.* [10, pp. 444–446], who also realized that in the particular case of two rectangular line-gratings the product comb (the comb of the Moiré) is in fact the Fourier series development of a trapezoidal (or triangular) periodic wave. This explains, back in the image domain, the trapezoidal (or triangular) profile shape of the Moiré between two binary gratings (see figure 3 (*a*)–(*f*) or figure 3 in [10]). But what Patorski *et al.* did not realize in their article is that this term-by-term multiplication of the original combs (i.e. the term-by-term product of the Fourier series of the two original gratings) can be interpreted according to the following theorem, which is the equivalent of the convolution theorem in the case of periodic functions [11, p. 36, 12, p. 166]:

*T-convolution theorem*

Let $f(x)$ and $g(x)$ be functions of period $T$ integrable on a one-period interval $(0, T)$, and let $\{F_n\}$ and $\{G_n\}$ (for $n = 0, \pm 1, \pm 2, \ldots$) be their Fourier series coefficients. Then the function

$$h(x) = \frac{1}{T}\int_0^T f(x - x')g(x')\,dx', \tag{9}$$

which is called the *T-convolution* of $f$ and $g$ and denoted by $f*g$ is also periodic with the same period $T$ and has Fourier series coefficients $\{H_n\}$ given by: $H_n = F_nG_n$ for all integers $n$.†

The $T$-convolution theorem can be rephrased, in a less rigorous but more illustrative way, as follows: if the spectrum of $f(x)$ is a comb with fundamental frequency of $1/T$ and impulse amplitudes $\{F_n\}$, and the spectrum of $g(x)$ is a comb with the same fundamental frequency and impulse amplitudes $\{G_n\}$, then the spectrum of the $T$-convolution $f*g$ is a comb with the same fundamental frequency and with impulse amplitudes of $\{F_nG_n\}$. In other words, the spectrum of the $T$-convolution of the two periodic images is the product of the combs in their respective spectra.

We would now like to apply this theorem to the case where $f(x)$ and $g(x)$ are the two given line gratings. Using this theorem, the fact that the comb of the $(1, -1)$-Moiré in the spectral domain is the term-by-term product of the combs of the two original gratings (Result 3.1) could be interpreted back in the image domain as follows:

The profile of the $(1, -1)$-Moiré generated in the superposition of two line-gratings with identical periods $T$ is the *T-convolution* of the two original line-gratings.‡

However, there still remains here a certain difficulty. The $T$-convolution theorem requires that $f(x)$ and $g(x)$ have the same period $T$, and moreover, the resulting $T$-convolution $f*g$ also has that same period. This requirement is necessary

† Note that $T$-convolution (also called *cyclic convolution*) is the periodic equivalent of the normal convolution with integration limits of $(-\infty, \infty)$, which cannot be used in the case of periodic functions (see [16], pp. 157–158). It is interesting to note that in general the normal convolution of a single period of $f$ with a single period of $g$ is *not* equal to a single period of the $T$-convolution $f*g$. Such an equality only occurs in cases in which the normal convolution of the two single periods is not longer than the period $T$; otherwise the outer ends which exceed the boundaries of each convolution period $T$ inevitably penetrate (additively) into the neighbouring periods in the $T$-convolution, thus generating a cyclic wrap-around effect which does not exist in the case of normal convolution. The discrete counterpart of the cyclic convolution is widely used in the discrete FT theory [8, p. 362].

‡ In fact, in the case of $(1, -1)$-Moiré it may be more appropriate to use the term *T-cross-correlation* between $f(x)$ and $g(x)$, which is defined, following [16, p. 172] as: $f(x)\bigstar g(x) = f(x)*g(-x)$. The reason is that in the case of $(1, -1)$-Moiré we have: $c_n = a_n^{(1)}a_{-n}^{(2)}$, which means that the second comb in the term-by-term multiplication is reflected about the origin, and therefore represents in the image domain the reflected image $g(-x)$; the resulting Moiré-profile is therefore the $T$-cross-correlation of $f(x)$ and $g(x)$. However, for the sake of consistency in the general case of the $(k_1, k_2, \ldots, k_N)$-Moiré, where some of the indices are positive and others are negative, we prefer to stick to the terminology of *T-convolution*, understanding that for any negative index in the list the image it represents must be reflected. In the common case where the original images are symmetric about the origin, the two terms coincide.

for the definition of the integral (9); or equivalently, from the spectral-domain point of view, this requirement is necessary since the comb multiplication in the spectrum is only meaningful if the two combs have a common support (i.e. their impulse locations in the spectrum coincide). However, in line-grating superpositions the original gratings may, of course, have different periods, and moreover, the resulting Moiré normally has yet a different period, $T_M$, which is given by equation (7). What happens then when $f(x)$, $g(x)$ and $f*g$ have different periods, $T_1$, $T_2$ and $T_M$?

From the spectral-domain point of view this difficulty is settled thanks to the complete independence between the impulse locations and the impulse amplitudes, as formulated by equations (3) and (4). The term-by-term multiplication of the combs in the spectrum only yields the *impulse amplitudes* of the resulting Moiré comb, but their actual *geometric locations* in the spectrum are determined, independently of the impulse amplitudes, by the frequencies and the angles of the superposed layers (i.e. by equation (3), or by its special case, equation (7)).

This difficulty can be also settled, in a more formal way, directly in the image domain, by the addition of a preliminary stage before the application of the $T$-convolution theorem. Before applying the theorem, the two original gratings must be *normalized*, i.e. stretched (and in the 2D case also rotated) in order that their periods coincide (or equivalently, in terms of the spectral domain: in order that their two combs have a common support). According to well-known results in the Fourier theory (see Appendix A) stretching and rotation of the original gratings do not affect the Fourier coefficients (impulse amplitudes) of their combs, but only their impulse locations in the spectrum. Therefore, according to Result 3.1, the amplitudes of the Moiré comb are not affected either by the normalization. This normalization, therefore, enables the theorem to be applied even to line-gratings with periods $T_1 \neq T_2$. Moreover, by selecting the new common period and angle of the two normalized gratings to coincide with the period and angle of the Moiré, as determined by equations (3) or (7), the resulting $T$-convolution received by the theorem will fit the actual period (and direction) of the Moiré. We can summarize the above discussion as follows.

*Result* 3.2

The profile of the $(1, -1)$-Moiré generated in the superposition of two line-gratings with periods $T_1$ and $T_2$ and an angle difference $\alpha$ can be seen from the image-domain point of view as a two-stage process:

(1) Normalization of the original gratings (by linear stretching- and rotation-transformations) in order to bring each of them to the period and the direction of the Moiré.
(2) $T$-convolution of the two normalized line-gratings. (This can be done by multiplying their combs in the spectrum and taking the inverse FT of the product.)

It is interesting to note that this result (for the special case of $T_1 = T_2$) has already been obtained by Harthong [13, pp. 30–31], using the theory of non-standard analysis.

Result 3.2 can be further generalized to also cover higher-order Moirés (as an illustration, refer to the second-order $(1, -2)$ Moiré shown in figure 5):

*Result* 3.3

The profile of the general $(k_1, k_2)$ Moiré generated in the superposition of two line-gratings with periods $T_1$ and $T_2$ and an angle difference $\alpha$ can be seen from the image-domain point of view as a normalized $T$-convolution of the images belonging to the $k_1$ subcomb of the first grating and to the $k_2$ subcomb of the second grating. In more detail, this can be seen as a three-stage process:

(1) Extracting the $k_1$ subcomb (i.e. the partial comb which contains only every $k_1$th impulse) from the comb of the first original line-grating, and similarly, extracting the $k_2$ subcomb from the comb of the second original grating.
(2) Normalization of the two subcombs by linear stretching- and rotation-transformations in order to bring each of them to the period and the direction of the Moiré, as they are determined by equation (3).
(3) $T$-convolution of the *images belonging to the two normalized subcombs*. (This can be done by multiplying the normalized subcombs in the spectrum and taking the inverse FT of the product.)

In conclusion, we see that thanks to the $T$-convolution theorem the duality between the image and the spectral domains is further extended to include the Moiré profiles as well. This enables us to present the extraction of the Moiré-profile between two gratings in either of the two domains. From the *spectral* point of view, the profile of any $(k_1, k_2)$ Moiré between two superposed ( = multiplied) gratings is obtained by extracting from their spectrum convolution only those impulses which belong to the $(k_1\, k_2)$ Moiré comb, thus reconstructing back in the image domain only the isolated contribution of this Moiré to the image of the superposition. On the other hand, from the point of view of the *image* domain, the profile form of any $(k_1, k_2)$ Moiré between two superposed gratings is a normalized $T$-convolution of the images belonging to the $k_1$ subcomb of the first grating and to the $k_2$ subcomb of the second grating.

The importance of the image-domain interpretation of the Moiré-profile as a $T$-convolution is not in the actual calculation of the profile, which is much more efficiently done in the spectral domain (as a term-by-term multiplication followed by an inverse FT). But as we will see later, this image-domain interpretation of the Moiré-profile will have an important role, thanks to the new light it sheds on the understanding of the Moirés and their envelope-forms.

## 4. Extension of the Moiré extraction to the general 2D case

We have seen above how the envelope form of a Moiré in the superposition of two line-gratings can be extracted from the Moiré-comb in the spectrum, or directly from the superposed images. How can this process be generalized to the superposition of doubly periodic images such as dot screens, where the Moiré effect in the superposition is really of a 2D nature (Moiré cells rather than Moiré bands)?

Let $f(x, y)$ be a doubly periodic image (for the sake of simplicity we assume that $f(x, y)$ is periodic in two orthogonal directions, $\theta_1$ and $\theta_1 + 90°$, with an identical period $T_1$ in both directions). Its spectrum $F(u, v)$ is a nailbed whose impulses are located on a regular lattice $L_1(u, v)$, rotated by the same angle $\theta_1$ and with period of $1/T_1$; the amplitude of a general $(k_1, k_2)$ impulse in this nailbed is given by the

coefficient of the $(k_1, k_2)$ harmonic term in the 2D Fourier series development of the periodic function $f(x, y)$.†

The lattice $L_1(u, v)$ can be seen as the 2D *support* of the 3D nailbed $F(u, v)$ on the plane of the spectrum, i.e. the set of all the nailbed impulse locations. Its unit points (0, 1) and (1, 0) are situated in the spectrum at the location vectors $\mathbf{f}_1$ and $\mathbf{f}_2$ of the two perpendicular fundamental impulses of the nailbed $F(u, v)$. Therefore the location $\mathbf{w}_1$ in the spectrum of a general point $(k_1, k_2)$ of this lattice is given by a linear combination of $\mathbf{f}_1$ and $\mathbf{f}_2$ with the integer coefficients $k_1$ and $k_2$; and the location $\mathbf{w}_2$ of the perpendicular point $(-k_2, k_1)$ on the lattice can also be expressed in a similar way:

$$\left.\begin{aligned} \mathbf{w}_1 &= k_1\mathbf{f}_1 + k_2\mathbf{f}_2, \\ \mathbf{w}_2 &= -k_2\mathbf{f}_1 + k_1\mathbf{f}_2. \end{aligned}\right\} \tag{10}$$

Let $g(x, y)$ be a second doubly periodic image whose periods in the two orthogonal directions $\theta_2$ and $\theta_2 + 90°$ are $T_2$. Again, its spectrum $G(u, v)$ is a nailbed whose support is a regular lattice $L_2(u, v)$, rotated by $\theta_2$ and with a period of $1/T_2$. Since the unit points (0, 1) and (1, 0) of the lattice $L_2(u, v)$ are situated in the spectrum at the location vectors $\mathbf{f}_3$ and $\mathbf{f}_4$ of the two perpendicular fundamental impulses of the nailbed $G(u, v)$, the location $\mathbf{w}_3$ of a general point $(k_3, k_4)$ of this lattice and the location $\mathbf{w}_4$ of its perpendicular twin $(-k_4, k_3)$ are given by

$$\left.\begin{aligned} \mathbf{w}_3 &= k_3\mathbf{f}_3 + k_4\mathbf{f}_4, \\ \mathbf{w}_4 &= -k_4\mathbf{f}_3 + k_3\mathbf{f}_4. \end{aligned}\right\} \tag{11}$$

Assume now that we superpose (i.e. multiply) $f(x, y)$ and $g(x, y)$. According to equations (1) and (2), the spectrum of the superposition is the convolution of the nailbeds $F(u, v)$ and $G(u, v)$; this means that a centred copy of one of the nailbeds is placed on top of each impulse of the other nailbed (the amplitude of each copied nailbed being scaled down by the amplitude of the impulse on top of which it has been copied). This convolution gives a 'forest' of impulses scattered throughout the spectrum, which are generally not even located on a common lattice (since the product of two periodic functions is generally not periodic, but rather *almost-periodic*; its spectrum is still impulsive, but its support is no longer a lattice and it may even be everywhere dense [14]). This is demonstrated in figure 6(*a*), which shows the locations of the impulses in the spectrum convolution, in a typical case where no Moiré effect is visible in the superposition (note that only impulses up to the third harmonic are shown).

Figure 6(*b*) and 6(*c*), however, show the impulse locations received in the spectrum convolution in typical cases in which the superposition does generate a visible Moiré effect, say a $(k_1, k_2, k_3, k_4)$ Moiré. As we can see, in these cases the d.c. impulse at the spectrum origin is closely surrounded by a whole cluster of impulses. The cluster impulses closest to the d.c. inside the visibility circle, are the $(k_1, k_2, k_3, k_4)$ impulse of the convolution, which is the fundamental impulse of the Moiré in question,‡ and its perpendicular counterpart, the $(-k_2, k_1, -k_4, k_3)$

† Obviously, some (or even most) of the impulses on the lattice $L(u, v)$ may have a zero amplitude: as in the case of $f(x, y) = \cos(x) + \cos(y)$, for instance.

‡ Note that this impulse is generated in the convolution by the $(k_1, k_2)$-impulse in the spectrum $F(u, v)$ of the first image and the $(k_3, k_4)$-impulse in the spectrum $G(u, v)$ of the second image.

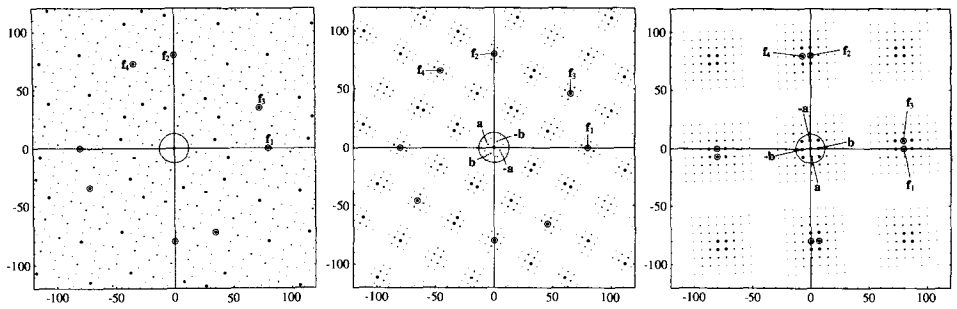


(*a*) (*b*) (*c*)

Figure 6. The spectrum of the superposition of two dot-screens with identical frequencies ($f_1 = f_2 = 80$) and with an angle difference of: (*a*) $\alpha = 22{\cdot}5°$; (*b*) $\alpha = 35°$; (*c*) $\alpha = 5°$. Only impulse locations are shown in the spectra, but not their amplitudes. Encircled points denote the locations of the fundamental impulses of the two original dot-screens. Large points represent convolution impulses obtained from the fundamental impulses of the original spectra (i.e. $(k_1, k_2, k_3, k_4)$ impulses with $k_i = 1, 0$, or $-1$); smaller points represent convolution impulses obtained from higher harmonics (only impulses up to the third harmonic are shown). The circle around the spectrum origin represents the visibility circle. Note that while in (*a*) no significant impulses are located inside the visibility circle, in (*b*) the spectrum origin is closely surrounded by the impulse-cluster of the $(1, 2, -2, -1)$ Moiré, and in (*c*) the spectrum origin is closely surrounded by the impulse-cluster of the $(1, 0, -1, 0)$ Moiré.

impulse, which is the fundamental impulse of the Moiré in the perpendicular direction. (Obviously, each of these two impulses is also accompanied by its respective symmetrical twin to the opposite side of the origin.) The locations of these four impulses are marked in figures 6 (*b*) and 6 (*c*) by: **a**, $-$**a**, **b** and $-$**b**. Note that in figure 6 (*b*) the impulse cluster belongs to the second order $(1, 2, -2, -1)$-Moiré, while in figure 6 (*c*) the impulse cluster belongs to the first order $(1, 0, -1, 0)$-Moiré, and consists of another subset of impulses from the spectrum convolution.

If we look attentively at the impulse cluster surrounding the d.c. we can see that this cluster is in fact a nailbed whose support is the regular lattice which is spanned by **a** and **b**, the locations of the fundamental Moiré impulses $(k_1, k_2, k_3, k_4)$ and $(-k_2, k_1, -k_4, k_3)$. This infinite impulse cluster represents in the spectrum the $(k_1, k_2, k_3, k_4)$-Moiré, and its basis vectors **a** and **b** (the locations of the fundamental impulses) determine the period and the two perpendicular directions of the Moiré. This impulse cluster is in fact the 2D generalization of the Moiré-comb that we had in section 3 (in the case of line-grating superpositions). We will call the infinite impulse cluster of the $(k_1, k_2, k_3, k_4)$-Moiré the $(k_1, k_2, k_3, k_4)$-*cluster*, and we will denote it by: $M_{k_1, k_2, k_3, k_4}(u, v)$. If we extract from the spectrum of the superposition only the impulses of this infinite cluster we get the 2D Fourier series development of the periodic envelope form of the $(k_1, k_2, k_3, k_4)$ Moiré; in other words, the amplitude of the $(i, j)$th impulse of the cluster is the coefficient of the $(i, j)$ harmonic term in the Fourier series development of the periodic Moiré envelope. By taking the inverse 2D FT of this extracted cluster we can analytically reconstruct in the image domain the envelope of this Moiré. If we denote the envelope of the $(k_1, k_2, k_3, k_4)$ Moiré between the superposed images $f(x, y)$ and $g(x, y)$ by $m_{k_1, k_2, k_3, k_4}(x, y)$, we therefore have

$$m_{k_1, k_2, k_3, k_4}(x, y) = \mathrm{FT}^{-1}\{M_{k_1, k_2, k_3, k_4}(u, v)\}.$$

The envelope (or intensity profile) of the $(k_1, k_2, k_3, k_4)$ Moiré between the superposed images $f(x, y)$ and $g(x, y)$ is therefore a function $m_{k_1,k_2,k_3,k_4}(x, y)$ in the image domain whose value at each point $(x, y)$ indicates quantitatively the intensity level of the Moiré in question, i.e. its particular intensity contribution to the image superposition. Note that although this Moiré is visible both in the image superposition $f(x, y)\,g(x, y)$ and in the extracted envelope $m_{k_1,k_2,k_3,k_4}(x, y)$, the latter does not contain the fine structure of the original images $f(x, y)$ and $g(x, y)$ but only the isolated form of the extracted $(k_1, k_2, k_3, k_4)$ Moiré; see for example the difference between figure 4 (*c*) (the image superposition) and figure 4 (*g*) (the extracted envelope of the (1, −1) Moiré). Moreover, in a single image superposition $f(x, y)\,g(x, y)$ there may be visible several different Moiré simultaneously; but each of them will have a different Moiré envelope $m_{k_1,k_2,k_3,k_4}(x, y)$ of its own.

It should be noted that the $(k_1, k_2, k_3, k_4)$ cluster exists in the spectrum convolution even is cases like figure 6 (*a*) where no Moiré effect is visible in the superposition. However in such cases the fundamental impulses $(k_1, k_2, k_3, k_4)$ and $(-k_2, k_1, -k_4, k_3)$ are located at a bigger distance from the d.c. beyond the visibility circle. Note that at the other extremity, when the $(k_1, k_2, k_3, k_4)$ Moiré reaches its singular point and its period becomes infinitely large (i.e. its frequency becomes zero), the whole infinite Moiré cluster around the spectrum origin collapses down on to the d.c. impulse.

Let us now find the expressions for the *location*, the *index* and the *amplitude* of the impulses of the $(k_1, k_2, k_3, k_4)$ Moiré cluster. If $\mathbf{a}$ is the location vector of the $(k_1, k_2, k_3, k_4)$ impulse in the convolution and $\mathbf{b}$ is the orthogonal location vector of the $(-k_2 k_1, -k_4, k_3)$ impulse, then we have according to the convolution rules (equation (3)):

$$\left.\begin{aligned}\mathbf{a} &= k_1\mathbf{f}_1 + k_2\mathbf{f}_2 + k_3\mathbf{f}_3 + k_4\mathbf{f}_4,\\ \mathbf{b} &= -k_2\mathbf{f}_1 + k_1\mathbf{f}_2 - k_4\mathbf{f}_3 + k_3\mathbf{f}_4.\end{aligned}\right\} \tag{12}$$

Since $\mathbf{a}$ and $\mathbf{b}$ are the basis vectors which span the lattice $L_M(u, v)$, the support of the Moiré cluster, the *location* of the $(i, j)$th impulse within this Moiré cluster is given by the linear combination $i\mathbf{a} + j\mathbf{b}$:

$$i\mathbf{a} + j\mathbf{b} = (ik_1 - jk_2)\mathbf{f}_1 + (ik_2 + jk_1)\mathbf{f}_2 + (ik_3 - jk_4)\mathbf{f}_3 + (ik_4 + jk_3)\mathbf{f}_4. \tag{13}$$

In terms of the impulse indices in the original nailbeds $F(u, v)$ and $G(u, v)$, the *index* of the $(i, j)$th impulse in the $(k_1, k_2, k_3, k_4)$ Moiré cluster is therefore

$$(ik_1 - jk_2, ik_2 + jk_1, ik_3 - jk_4, ik_4 + jk_3). \tag{14}$$

This means that the $(k_1, k_2, k_3, k_4)$ Moiré cluster is the subset of the full spectrum-convolution which only contains those impulses whose indices are of the type (14).

Finally, the *amplitude* $c_{i,j}$ of the $(i, j)$th impulse in the $(k_1, k_2, k_3, k_4)$ Moiré cluster is given by

$$c_{i,j} = a_{ik_1 - jk_2, ik_2 + jk_1, ik_3 - jk_4, ik_4 + jk_3},$$

and according to the convolution rules (equation (4)) we get

$$c_{i,j} = a^{(1)}_{ik_1 - jk_2} a^{(2)}_{ik_2 + jk_1} a^{(3)}_{ik_3 - jk_4} a^{(4)}_{ik_4 + jk_3}.$$

But since we are dealing here with the superposition of two orthogonal layers (dot screens) rather than with a superposition of four independent layers (gratings),

it is more meaningful to group these amplitudes in pairs, so that each component corresponds to an impulse amplitude in the nailbed $F(u,v)$ or $G(u,v)$:

$$c_{i,j} = a^{(f)}_{ik_1 - jk_2,\, ik_2 + jk_1} a^{(g)}_{ik_3 - jk_4,\, ik_4 + jk_3}. \tag{15}$$

This means that the amplitude $c_{i,j}$ of the $(i,j)$th impulse in the $(k_1, k_2, k_3, k_4)$ Moiré cluster is the product of the amplitudes of its two generating impulses: the $(ik_1 - jk_2, ik_2 + jk_1)$ impulse of the nailbed $F(u,v)$ and the $(ik_3 - jk_4, ik_4 + jk_3)$ impulse of the nailbed $G(u,v)$. This can be interpreted more illustratively in the following way.

Let us call the $(k_1, k_2)$ *subnailbed of the nailbed* $F(u,v)$ the partial nailbed of $F(u,v)$ whose fundamental impulses are the $(k_1, k_2)$ and the $(-k_2, k_1)$ impulses of $F(u,v)$; its general $(i,j)$ impulse is the $i(k_1, k_2) + j(-k_2, k_1) = (ik_1 - jk_2, ik_2 + jk_1)$ impulse of $F(u,v)$. Similarly, let the $(k_3, k_4)$ subnailbed of the nailbed $G(u,v)$ be the partial nailbed of $G(u,v)$ whose fundamental impulses are the $(k_3, k_4)$ and the $(-k_4, k_3)$ impulses of $G(u,v)$; its general $(i,j)$ impulse is the $(ik_3 - jk_4, ik_4 + jk_3)$ impulse of $G(u,v)$. It therefore follows from (15) that the amplitude of the $(i,j)$ impulse of the nailbed of the $(k_1, k_2, k_3, k_4)$ Moiré in the spectrum convolution is the product of the $(i,j)$ impulse of the $(k_1, k_2)$ subnailbed of $F(u,v)$ and the $(i,j)$ impulse of the $(k_3, k_4)$ subnailbed of $G(u,v)$. This means that:

*Result* 4.1 (*2D generalization of Result 3.1*)

The impulse amplitudes of the $(k_1, k_2, k_3, k_4)$ Moiré cluster in the spectrum-convolution are the term-by-term product of the $(k_1, k_2)$ subnailbed of $F(u,v)$ and the $(k_3, k_4)$ subnailbed of $G(u,v)$.

For example, in the case of the simplest first-order Moiré between the images $f(x,y)$ and $g(x,y)$, the $(1, 0, -1, 0)$ Moiré (see figure 6(*c*)), the amplitudes of the Moiré cluster impulses in the spectrum-convolution are given by: $c_{i,j} = a^{(f)}_{i,j} a^{(g)}_{-i,-j}$. This means that in this case the Moiré cluster is simply a term-by-term product of the nailbeds $F(u,v)$ and $G(-u,-v)$ of the original images $f(x,y)$ and $g(-x,-y)$. For the second-order $(1, 2, -2, -1)$ Moiré (see figure 6(*b*)) the amplitudes of the Moiré cluster impulses are: $c_{i,j} = a^{(f)}_{i-2j,\, 2i+j} a^{(g)}_{-2i+j,\, -i-2j}$.

Now, since we also know the exact *locations* of the impulses of the Moiré cluster (according to equations (3) or (5)–(6)), the spectrum of the isolated Moiré in question is fully determined, and given analytically by

$$M_{k_1,k_2,k_3,k_4}(u,v) = \sum_{i=-\infty}^{\infty} \sum_{j=-\infty}^{\infty} c_{i,j} \delta_{i\mathbf{a}+j\mathbf{b}}(u,v),$$

where $\delta_{\mathbf{f}}(u,v)$ denotes an impulse (Dirac function) located at the frequency vector $\mathbf{f}$ in the spectrum. Therefore, we can reconstruct the envelope-form of the Moiré, back in the image domain, by formally taking the inverse FT of the isolated Moiré cluster. Practically this can be done either by interpreting the Moiré cluster as a 2D Fourier series, and summing up the corresponding sinusoidal functions (up to the desired precision); or, more efficiently, by approximating the continuous inverse FT of the isolated Moiré cluster by means of the inverse 2D discrete FT (using fast FT).

Like in the case of grating superposition (section 3), the spectral domain term-by-term multiplication of the Moiré clusters can be interpreted directly in the image domain by means of the 2D version of the $T$-convolution theorem:

*2D T-convolution theorem*

Let $f(x, y)$ and $g(x, y)$ be doubly periodic functions of period $T_x$, $T_y$ integrable on a one-period interval ($0 \leqslant x \leqslant T_x$, $0 \leqslant y \leqslant T_y$), and let $\{F_{m,n}\}$ and $\{G_{m,n}\}$ (for $m, n = 0, \pm 1, \pm 2, \ldots$) be their 2D Fourier series coefficients. Then the function

$$h(x, y) = \frac{1}{T_x T_y} \int_0^{T_x} \int_0^{T_y} f(x - x', y - y') g(x', y') \, dx' \, dy', \tag{16}$$

which is called the *T-convolution* of $f$ and $g$ and denoted by $f{**}g$ is also doubly periodic with the same periods $T_x$, $T_y$ and has Fourier series coefficients $\{H_{m,n}\}$ given by: $H_{m,n} = F_{m,n} G_{m,n}$ for all integers $m, n$.

According to this theorem we have the following result, which is the generalization of Result 3.3 to the general 2D case.

*Result* 4.2

The envelope-form of the $(k_1, k_2, k_3, k_4)$ Moiré in the superposition of $f(x, y)$ and $g(x, y)$ is a $T$-convolution of the (normalized) images belonging to the $(k_1, k_2)$ subnailbed of $F(u, v)$ and the $(k_3, k_4)$ subnailbed of $G(u, v)$. Note that, before applying the $T$-convolution theorem, the images must be normalized by stretching and rotation transformations, to fit the actual period and angle of the Moiré, as determined by equation (3) (or by the lattice $L_M(u, v)$ of the $(k_1, k_2, k_3, k_4)$ Moiré, which is spanned by the fundamental vectors **a** and **b**). As shown in Appendix A, normalizing the periodic images by stretching and rotation does not affect their impulse amplitudes in the spectrum, but only the impulse locations.

These results can be easily generalized to any $(k_1, k_2, \ldots, k_N)$ Moiré between any number of superposed images by a simple straightforward extension of this procedure.

## 5. The special case of the (1, 0, −1, 0) Moiré

In this section we will apply the results obtained above to the special case of the $(1, 0, -1, 0)$ Moiré. We will see in particular how they explain the several striking visual effects observed in superpositions of two dot-screens with identical periods and a small angle difference (like in figure 1), which are clearly cases of $(1, 0, -1, 0)$ Moiré.

As we have seen in the example following Result 4.1, in the special case of the $(1, 0, -1, 0)$ Moiré the impulse amplitudes of the Moiré cluster are simply a term-by-term product of the nailbeds $F(u, v)$ and $G(-u, -v)$ themselves: $c_{i,j} = a^{(f)}_{i,j} a^{(g)}_{-i,-j}$. Since the impulse locations of this Moiré cluster are also known (according to equation (3)), we can obtain the envelope of the $(1, 0, -1, 0)$ Moiré by extracting this Moiré cluster from the full-spectrum-convolution, and taking its inverse FT.

However, according to Result 4.2 (based on the 2D $T$-convolution theorem), the envelope of the $(1, 0, -1, 0)$ Moiré can also be interpreted directly in the image domain: in this special case the Moiré envelope is simply a $T$-convolution of the original images $f(x, y)$ and $g(-x, -y)$ (after undergoing the necessary stretching and rotations to make their periods, or their supporting lattices in the spectrum, coincide). This result has been previously derived by Harthong [13, p. 69], using sophisticated mathematical tools such as non-standard analysis; as we can see, this result is obtained here (for any doubly periodic images $f(x, y)$, $g(x, y)$) as a simple particular case of our generalized Moiré extraction method.

It should be noted here that when the superposed images are dot-screens it may be tempting to say that the form of a single 2D period of the $(1, 0, -1, 0)$ Moiré is given by a (normalized) convolution of a single dot ( = 2D period) of the first screen with a single dot of the second screen. However, this statement is only correct when the convolution of the two single dots does not exceed the size of a single 2D period ($T_x \times T_y$); otherwise the outer ends of the neighbouring convolution periods inevitably penetrate (additively) into the area of the current period. This cyclical wrap-around effect is automatically taken care of by $T$-convolution, but not by the simple convolution of single screen-dots.

Let us see now how the above $T$-convolution theory sheds a new light on the Moiré envelopes, and explains the striking visual effects observed in superpositions of dot-screens with any desired dot shapes, such as in figures 1 (*a*)–(*d*). In all of these figures the Moiré is obtained by superposing two dot-screens having identical frequencies, with just a small angle difference $\alpha$; this implies that in all of these cases we are dealing, indeed, with a $(1, 0, -1, 0)$ Moiré.

### 5.1. *The forms of the Moiré cells*

#### 5.1.1. *Case 1*

As we see in the figures, the form of the Moiré cells in the superpositions is most clear-cut and striking where one of the two screens is relatively dark (see for example figure 7 (*a*) and (*b*)). This happens because the dark screen includes only tiny white dots, which play in the $T$-convolution the role of very narrow impulses with amplitude 1. As we can see in figure 8 (*a*), the $T$-convolution of such impulses and dots of any shape (from the second screen) gives dots of the latter shape, in which the zero values remain at zero, the 1 values are scaled down to the value $A$ (the volume or the area of the narrow white impulse divided by the total cell area, $T_x \times T_y$), and the sharp step transitions are replaced by slightly softer ramps. This means that the dot shape received in the normalized Moiré-period is practically identical to the dot shape of the second screen, except that its white areas turn darker. However, this normalized Moiré period is stretched back into the real size of the Moiré period $T_M$, as it is determined by equations (5–6) (or in our case, according to equation (8) by the angle difference $\alpha$ alone, since the screen frequencies are fixed; note that the Moiré period becomes larger as the angle $\alpha$ tends to 0°). This means that the Moiré form in this case is essentially a magnified version of the second screen, where the magnification rate is controlled only by the angle $\alpha$. This interesting magnification property of the Moiré effect can be used in certain applications as a 'virtual microscope' for visualizing the detailed structure of a given screen.

#### 5.1.2. *Case 2*

A similar, albeit somewhat less impressive, effect occurs in the superposition where one of the two screens contains tiny *black* dots (see figure 7 (*c*) and (*d*)). Tiny black dots on a white background can be interpreted as 'inversed' impulses of 0 amplitude on a constant background of amplitude 1. As we can see in figure 8 (*b*), the $T$-convolution of such inversed impulses and dots of any shape (from the second screen) gives dots of the latter shape, where the zero values are replaced by the value $B$ (the volume under a one-period cell of the second screen divided by $T_x \times T_y$) and the 1 values are replaced by the value $B - A$ (where $A$ is the volume of the 'hole' of the narrow black impulse divided by $T_x \times T_y$). This means that the dot shape of

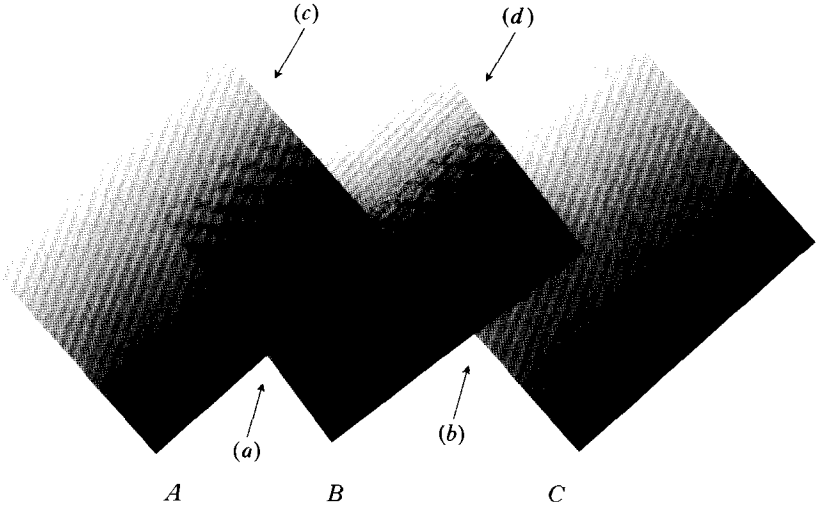


Figure 7. Demonstration of the magnification and rotation properties of the $(1, 0, -1, 0)$ Moiré between two dot-screens. Dot-screen $B$ consisting of black '1'-shaped dots is superposed with two identical dot-screens of black circular dots, $A$ and $C$. Each of the three screens consists of gradually increasing dots with identical frequencies; the superposition angle is 4°. It can be seen that: (*a*), (*b*): where one of the two superposed screens is relatively dark and consists of tiny white dots, the Moiré envelope-form is essentially a magnified version of the other screen; (*c*), (*d*): where one of the two superposed screens consists of tiny black dots, the Moiré envelope form is essentially a magnified, inverse-video version of the other screen. Note that in both cases the orientation of the 'l'-shaped Moiré is almost perpendicular to that of the original 'l'-shaped dots of screen $B$. Note also the gradual Moiré form transitions between (*a*) and (*c*) and between (*b*) and (*d*), through all the intermediate, blurred stages.

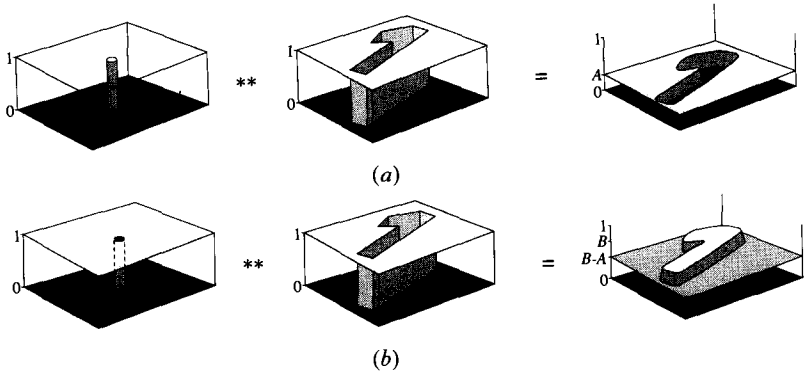


Figure 8. (*a*) The $T$-convolution of tiny white dots (from the first screen) with dots of any given shape (from the other screen) gives dots of essentially the same given shape. (*b*) The $T$-convolution of tiny black dots (from the first screen) with dots of any given shape (from the other screen) gives dots of essentially the same shape, but in inverse video.

the normalized Moiré period is similar to the dot shape of the second screen, except that it appears in inverse video and with slightly softer ramps. And indeed, looking at figures 1 and 7, we see that wherever one of the screens in the superposition contains tiny black dots, the Moiré appears to be a magnified version of the other screen, but this time in inverse video.

Note that although the amplitude difference in both of the cases above is identical (in both cases it equals $A$), the perceived contrast in the first case appears to the eye quite stronger than in the second one. The reason for this phenomenon is that the response (or sensibility) of the human visual system to light intensity is not linear in its nature, but rather close to logarithmic [15, pp. 27–29]. If we plot the intensities or the Moiré profiles logarithmically, i.e. in terms of density rather than in terms of reflectance, we get a more realistic representation of the perceptual contrast of the Moiré, which corresponds better to human perception (see figure 3 (*g*)–(*i*)).

5.1.3. *Case 3*

When none of the two superposed screens contains tiny dots (either white or black), the envelope form of the resulting Moiré is still a magnified version of the $T$-convolution of the two original screens. This $T$-convolution gives, as before, some kind of blending between the two original dot shapes, but this time the resulting shape has a rather blurred or smoothed appearance and the Moiré looks less attractive to the eye. Note in figures 1 (*a*)–(*d*) the sharp-cut Moiré envelopes at the bottom and at the top ends of the superposed area (where the white or black tiny dots are located), and the gradual transition between them through all the intermediate, blurred stages (where none of the screens contains tiny dots).

Another interesting example of this type occurs when two screens with circular black dots are superposed, unlike in figure 1 (*a*), with their grey levels (dot sizes) in match (see figure 9). In this case the resulting Moiré envelope form is no longer mostly circular, as it was in figure 1 (*a*), but rather has a squarish form at the darker grey levels. This reflects the forms obtained by $T$-convolution of two periodic screens with identical, black circular dots; indeed, these forms tend to become squarish as the circular dots increase, due to the cyclical wrap-around effect caused at the four boundaries of the period cell. This can be verified by actually calculating the $T$-convolution. Note that 2D $T$-convolutions of periodic images on the

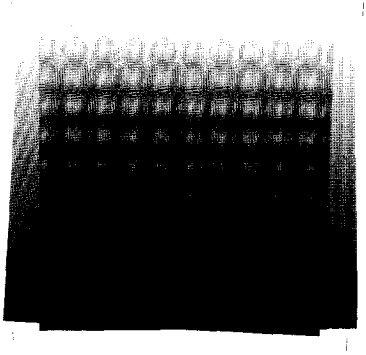

Figure 9. Two circular black screens which are superposed, unlike in figure 1 (*a*), with matching grey levels (dot sizes). The Moiré envelope form in this case is no longer circular as in figure 1 (*a*), but rather has a squarish form in the darker grey levels.

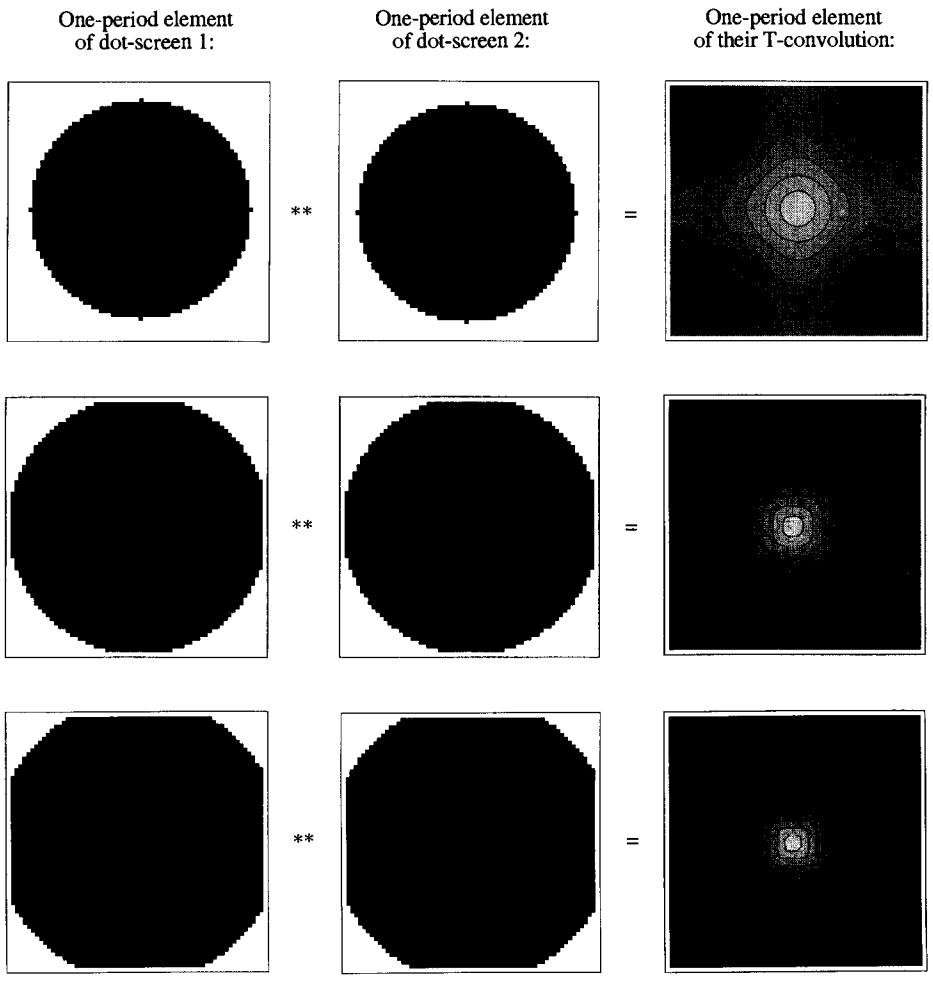


Figure 10. $T$-convolution of two identical, circular black dot screens: each row shows the $T$-convolution at a different grey level (screen dot size). The $T$-convolution in each of the rows is calculated digitally by multiplying the fast FTs of the two screen elements and taking the inverse fast FT of their product. It clearly appears that at higher grey levels the forms received by the $T$-convolution are rather squarish; this agrees perfectly with the Moiré envelope forms actually obtained in the screen superposition (figure 9) at the respective grey levels.

continuous $(x, y)$ plane (or rather, their discretized approximations) can be easily performed in a computer program by using 2D discrete FT: since the discrete FT is inherently periodic, it follows that the discrete convolution obtained by using it (i.e. by multiplying the discrete FTs of one-period cells of the original screens and taking the inverse discrete FT of the product) is also periodic and cyclic [8, p. 362]; this is, indeed, the discrete counterpart of $T$-convolution. Figure 10 shows the $T$-convolution obtained in this manner for the case of two identical black circular dots of various sizes; these results are identical to the Moiré-forms obtained at the corresponding grey levels in figure 9.

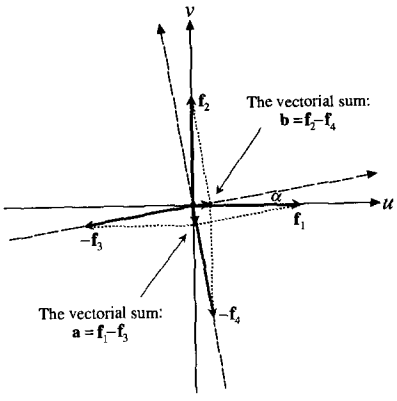


Figure 11. A detail from figure 6 (*c*) showing the spectral interpretation of the $(1,0,-1,0)$ Moiré between two dot-screens with identical frequencies and a small angle difference $\alpha$ (for the sake of clarity the angle $\alpha$ is shown here slightly larger than in figure 6 (*c*)). It is clearly seen that the low frequency vectorial sums **a** and **b** (which represent the impulse locations of the two fundamental impulses of the $(1,0,-1,0)$ Moiré cluster) are closely perpendicular to the directions of the two original screens: **a** is closely perpendicular to $\mathbf{f}_1$ and $\mathbf{f}_3$, and **b** is almost perpendicular to $\mathbf{f}_2$ and $\mathbf{f}_4$.

5.2. *The orientation of the Moiré cells*

As we can see in figure 7, although the $(1,0,-1,0)$ Moiré cells inherit the forms of the original screen cells, they do not inherit their orientation. Rather than having the same direction as the cells of the original screens (or an intermediate orientation), the Moiré cells appear in a perpendicular direction. This fact may seem surprising at first, but in fact it can easily be understood using the theory developed in section 4.

As we have seen, the orientation of the Moiré is determined by the location of the fundamental impulses of the Moiré cluster in the spectrum, i.e. by the location of the basis vectors **a** and **b** (equation (12)). In the case of the $(1,0,-1,0)$ Moiré these vectors are reduced to

$$\left.\begin{aligned}\mathbf{a}&=\mathbf{f}_1-\mathbf{f}_3,\\ \mathbf{b}&=\mathbf{f}_2-\mathbf{f}_4.\end{aligned}\right\}$$

And in fact, as we can see in figures 6 (*c*) and 11, when the two original screens have the same frequency, these basis vectors are rotated by about 90° from the directions of the frequency vectors $\mathbf{f}_i$ of the two original screens. This means that the $(1,0,-1,0)$ Moiré cluster (and the Moiré envelope form it generates in the image domain) are rotated by about 90° relative to the original screens $f(x,y)$ and $g(x,y)$. Note that the precise period and angle of this Moiré can be found by formulas (8) which were derived for the $(1,-1)$ Moiré between two line-gratings with identical periods $T$ and angle difference of $\alpha$.

Obviously, the fact that the direction of the Moiré envelope is almost perpendicular to the direction of the original screens is a property of the $(1,0,-1,0)$ Moiré between two screens having identical frequencies; in other cases the angle of the Moiré may be different. In all cases the Moiré angle can be found by equations (5)–(6).

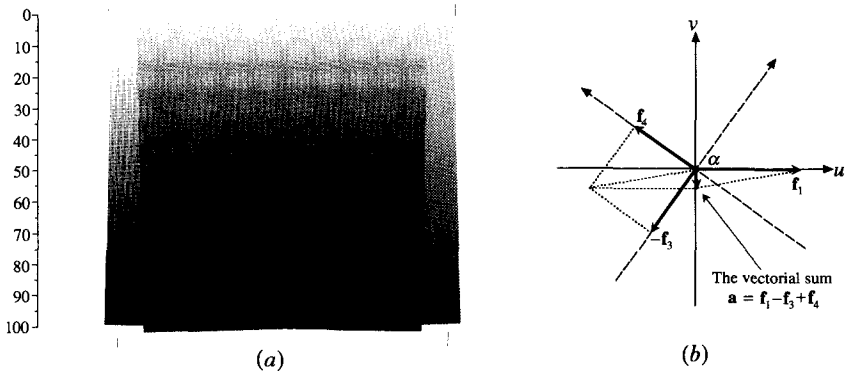


(*a*) (*b*)

Figure 12. (*a*) The $(1, 0, -1, 1)$ Moiré between two dot screens of gradually increasing black circular dots, whose frequency ratio is $f_1/f_3 = \sqrt{2} = 1{\cdot}4142$ and whose angle difference $\alpha$ is close to 45°. (*b*) The spectral interpretation of the Moiré in question (for the sake of clarity, only the frequency vectors in one of the two perpendicular directions are shown). The low frequency vectorial sum **a** is the impulse location of one of the two perpendicular fundamental impulses of the $(1, 0, -1, 1)$ Moiré impulse cluster.

## 6. The case of more complex and higher order Moirés

As we have seen in section 4 above, the general Moiré case differs from the elementary $(1, 0, -1, 0)$-Moiré in that in Result 4.2 the $(k_1, k_2)$ subnailbed of $F(u, v)$ and the $(k_3, k_4)$ subnailbed of $G(u, v)$ no longer coincide with the nailbeds $F(u, v)$ and $G(u, v)$ themselves. Equivalently, from the image domain point of view, the Moiré envelope is no longer a (normalized) $T$-convolution of the original images $f(x, y)$ and $g(x, y)$ themselves, but rather a $T$-convolution of their derived images $f'(x, y)$ and $g'(x, y)$, whose spectra are the $(k_1, k_2)$ subnailbed of $F(u, v)$ and the $(k_3, k_4)$ subnailbed of $G(u, v)$. This means that in the general case the envelope form of the $(k_1, k_2, k_3, k_4)$ Moiré cannot be expected to reflect the original forms of the screen elements, but rather a more complex relationship between them.

We will demonstrate this using the case of the $(1, 0, -1, 1)$ Moiré, which occurs between two dot-screens (of circular black dots) with a frequency ratio of $\sqrt{2} = 1{\cdot}4142$ and an angle difference $\alpha$ close to 45° (see figures 12 (*a*), (*b*)). In this case the Moiré cluster which surrounds the spectrum origin has the basis vectors

$$\left.\begin{aligned} \mathbf{a} &= \mathbf{f}_1 - \mathbf{f}_3 + \mathbf{f}_4, \\ \mathbf{b} &= \mathbf{f}_2 - \mathbf{f}_3 - \mathbf{f}_4, \end{aligned}\right\}$$

and according to equation (14) it contains all the impulses of the full nailbed-convolution whose indices are of the type: $(i, j, -i-j, i-j)$.

Figure 13 shows this Moiré cluster for two different grey-level combinations of the original dot screens, and the Moiré envelopes obtained by taking the inverse FT of each of these spectra. As we can see, these results accurately predict the Moiré envelope forms actually obtained in the screen superposition (figure 12) at the corresponding grey levels.

Note that, in general, the more complex the Moiré (that is, the more superposed screens it contains, or the higher its $k_i$ indices or harmonics are), the more blurred, low-contrast and washed-out its envelope-form looks. The most visually impressive Moiré envelope forms are normally obtained in low-order Moirés between few superposed layers.

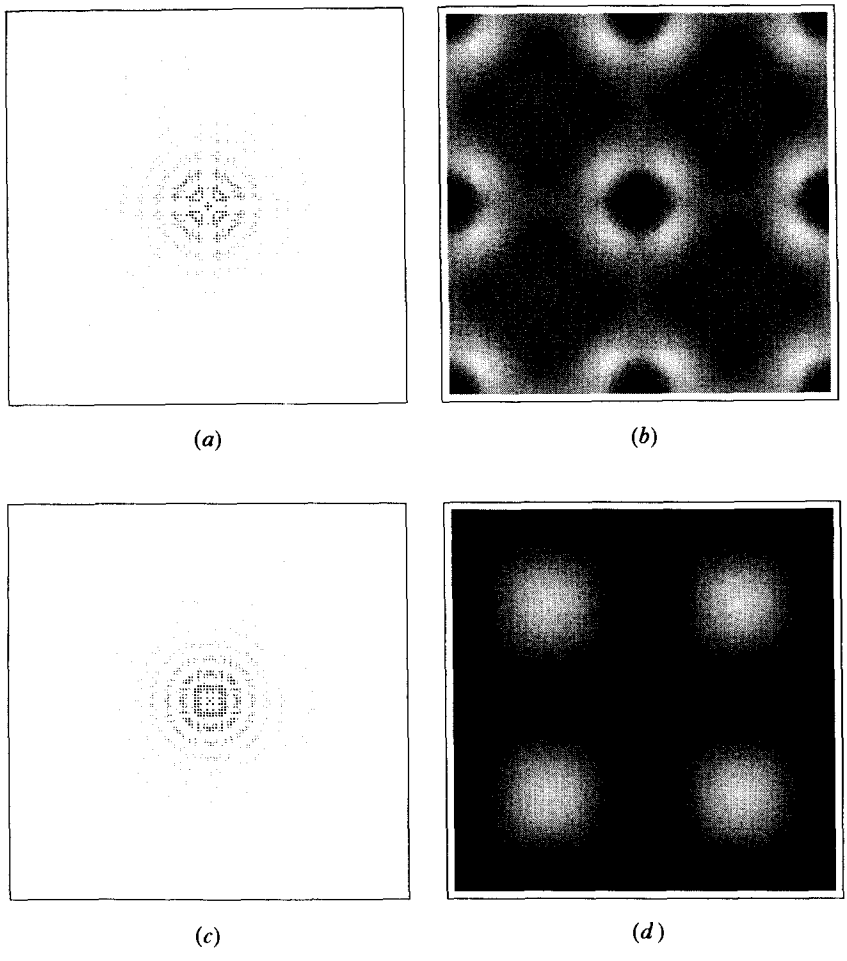


Figure 13. Left images: the impulse-cluster of the $(1, 0, -1, 1)$ Moiré between two identical dot-screens with circular black dots, analytically calculated (up to 50 harmonics) for two different dot sizes (screen grey levels). Right images: reconstruction of the corresponding Moiré-envelopes, obtained by taking the inverse fast FT of each of these spectra. Note that these results agree perfectly with the Moirés actually obtained in the screen superposition at the respective grey levels (levels 55 and 70 on the scale at figure 12).

## 7. Conclusions

The Moiré envelope (or intensity profile) is a very important notion in the Moiré theory, since it represents quantitatively (and not only qualitatively) the given Moiré in the image superposition. In this article we show how, by using the $T$-convolution theorem, the duality between the image and the spectral domains can be further extended to include also the Moiré envelopes. This enables us to present the envelope extraction of any Moiré between superposed screens in either of the two domains. From the *spectral* point of view, the envelope of any $(k_1, k_1, k_3, k_4)$ Moiré between two superposed ( = multiplied) screens is obtained by extracting from their spectrum convolution only those impulses which belong to the $(k_1, k_2, k_3, k_4)$ Moiré cluster, thus reconstructing back in the image domain only the

isolated contribution of this Moiré to the image of the superposition. On the other hand, from the point of view of the *image* domain, the envelope form of any $(k_1, k_2, k_3, k_4)$ Moiré between two superposed screens is a normalized $T$-convolution of the images belonging to the $(k_1, k_2)$ subnailbed of the first screen and to the $(k_3, k_4)$ subnailbed of the second screen.

Illustrating these results for the simple case of the $(1, 0, -1, 0)$ Moiré between two screens, we show that in this particular case the envelope form of the Moiré is a magnified version of the $T$-convolution of the two original screens; and if the two screens have identical frequencies, the magnification rate is only controlled by the superposition angle $\alpha$. In particular, when one of the screens is relatively dark and consists of tiny white dots, the Moiré form is essentially a magnified version of the other screen; and when one of the screens consists of tiny black dots the Moiré envelope is a magnified inverse-video version of the other screen.

Although our analysis method is presented in this article for the case of two superposed layers (line-gratings or dot-screens), it is completely general and it can be used for deriving the envelope form of any order Moirés between any number of superposed layers.

**Acknowledgments**

I would like to thank Mr Ph. Vosseler and Mr C. Waeber of the DE, EPFL for their assistance in the generation of the high-resolution films used for the figures of the screen superpositions.

## Appendix A

We used in this article the fact that stretching and rotating a periodic (or doubly periodic) image does not affect the *impulse amplitudes* of its comb (or nailbed), but only their *impulse locations* in the spectrum. In this Appendix we show how these properties can be derived, based on well-known results in the Fourier theory. We will use here the letters $p$ and $P$ to denote a periodic function and its spectrum, and the letters $f$ and $F$ to denote an arbitrary function (not necessarily periodic) and its spectrum.

### A.1. *Invariance of 2D FT under rotation*

This property of 2D FT is valid for any function: if $f(x, y)$ is rotated by angle $\theta$, its spectrum $F(u, v)$ is also rotated by the same angle. This invariance of the 2D FT under rotation is a special case of its more complex behaviour under a general linear transformation, which is given for instance in [16, p. 308].

### A.2. *Invariance of 2D FT of periodic functions under scaling*

According to the similarity theorem [8, p. 244], for any function $f(x, y)$ with FT $F(u, v)$ we have

$$f(ax, by) \leftrightarrow \frac{1}{|ab|} F\left(\frac{u}{a}, \frac{v}{b}\right). \tag{A 1}$$

However, a special case of interest occurs with periodic functions, where the spectrum is impulsive; in this case the factor $1/|ab|$ is cancelled out, and we have [8, p. 103]

$$p(ax, by) \leftrightarrow P\left(\frac{u}{a}, \frac{v}{b}\right). \tag{A 2}$$

This is normally formulated in the following way (see, for example, the 1D equivalent in [17, pp. 59–61]):

Let the function $p(x, y)$ be periodic with periods $T_x, T_y$ and generate the Fourier series

$$p(x,y) \rightarrow \sum_{m=-\infty}^{\infty} \sum_{n=-\infty}^{\infty} a_{m,n} \cos 2\pi\left(\frac{mx}{T_x} + \frac{ny}{T_y}\right) + \sum_{m=-\infty}^{\infty} \sum_{n=-\infty}^{\infty} b_{m,n} \sin 2\pi\left(\frac{mx}{T_x} + \frac{ny}{T_y}\right).$$

Then $p(ax, by)$ is periodic with periods $T_x/a$, $T_y/b$, and the Fourier series it generates preserves the same coefficients (impulse amplitudes) $a_{m,n}$ and $b_{m,n}$:

$$p(ax, by) \rightarrow \sum_{m=-\infty}^{\infty} \sum_{n=-\infty}^{\infty} a_{m,n} \cos 2\pi\left(\frac{mx}{T_x/a} + \frac{ny}{T_y/b}\right) + \sum_{m=-\infty}^{\infty} \sum_{n=-\infty}^{\infty} b_{m,n} \sin 2\pi\left(\frac{mx}{T_x/a} + \frac{ny}{T_y/b}\right).$$

## References


[1] OSTER, G., 1969, *The Science of Moiré Patterns*, second edition (Edmund Scientific).
[2] NISHIJIMA, Y., and OSTER, G., 1964, *J. Opt. Soc. Am.*, **54,** 1.
[3] YULE, J. A. C., 1967, *Principles of Color Reproduction* (New York: Wiley), Chap. 13, pp. 328–345.
[4] AMIDROR, I., 1991, *Raster Imaging and Digital Typography II, Proceedings of the Second International Conference on Raster Imaging and Digital Typography*, edited by R. A. Morris and J. André (Cambridge University Press), pp. 98–119.
[5] OSTER, G., WASSERMAN, M., and ZWERLING, C., 1964, *J. Opt. Soc. Am.*, **54,** 169.
[6] BRYNGDAHL, O., 1975, *J. Opt. Soc. Am.*, **65,** 685.
[7] ROSENFIELD, A., and KAK, A. C., 1982, *Digital Picture Processing*, second edition Vol. 1 (Florida: Academic).
[8] BRACEWELL, R. N., 1986, *The Fourier Transform and its Applications*, second edition (Reading, NY: McGraw-Hill).
[9] ULICHNEY, R., 1988, *Digital Halftoning* (Cambridge, MA: MIT Press).
[10] PATORSKI, K., YOKOZEKI, S., and SUZUKI, T., 1976, *Japanese Journal of Applied Physics*, **15,** 443.
[11] ZYGMUND, A., 1968, *Trigonometric Series* Vol. 1 (Cambridge: Cambridge University Press).
[12] CHAMPENEY, D. C., 1987, *Fourier Theorems* (Cambridge: Cambridge University Press).
[13] HARTHONG, J., 1981, *Adv. Appl. Math.*, **2,** 24.
[14] BREDIKHINA, E. A., 1988, *Encyclopaedia of Mathematics*, vol. 1 (Dordrecht: Kluwer), pp. 154–156.
[15] PRATT, W. K., *Digital Image Processing*, 1991, second edition (New York: Wiley).
[16] GASKILL, J. D., 1978, *Linear Systems, Fourier Transforms, and Optics* (New York: Wiley).
[17] CARTWRIGHT, M., 1990, *Fourier Methods for Mathematicians, Scientists and Engineers* (Chichester, UK: Ellis Horwood).